AD-A099 782 NAVAL UNDERWATER SYSTEMS CENTER NEW LONDON CT NEW LO--ETC F/6 17/1
A TOWABLE, MOVING-COIL ACOUSTIC TARGET FOR LOW FREQUENCY ARRAY --ETC(U)
APR 81 B S WILLARD

UNCLASSIFIED NUSC-TR-6369 NL

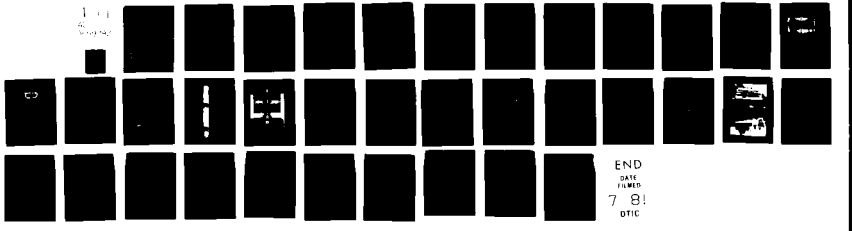

END
DATE FILMED
7 81
DTIC

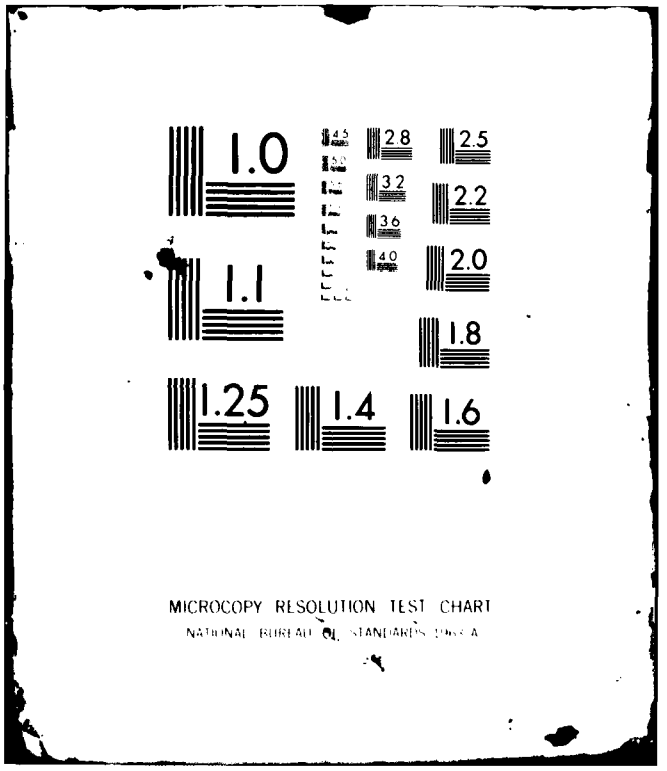
1.0
1.1
1.25
1.4
1.6
1.8
2.0
2.2
2.5
2.8
3.2
3.6
4.0
MICROCOPY RESOLUTION TEST CHART
NATIONAL BUREAU OF STANDARDS 1963-A

NUSC Technical Report 6369
29 April 1981

LEVEL II

A Towable, Moving-Coil Acoustic Target For Low Frequency Array Calibration

Bernard S. Willard
Submarine Sonar Department

Naval Underwater Systems Center
Newport, Rhode Island / New London, Connecticut

Preface

This research was conducted under NUSC IR/IED Project No. F61512, "Low Frequency Sound Sources for Array Evaluation," Principal Investigator, B. Willard (Code 3231).

The technical reviewers for this report were Dr. C. Sherman (Code 323) and Dr. R. Woollett (Code 323).

Reviewed and Approved: 29 April 1981

W. A. Von Winkle

W. A. Von Winkle
Associate Director for Science and Technology

The author of this report is located at NUSC's
Fort Lauderdale Detachment, 1650 SW 39 St.,
Fort Lauderdale, FL 33315.

REPORT DOCUMENTATION PAGE

READ INSTRUCTIONS BEFORE COMPLETING FORM

1. REPORT NUMBER: TR 6369	2. GOVT ACCESSION NO.: AD-A099 782
3. RECIPIENT'S CATALOG NUMBER:	
4. TITLE (and Subtitle): A TOWABLE, MOVING-COIL ACOUSTIC TARGET FOR LOW FREQUENCY ARRAY CALIBRATION •	5. TYPE OF REPORT & PERIOD COVERED:
	6. PERFORMING ORG. REPORT NUMBER:
7. AUTHOR(s): Bernard S. Willard	8. CONTRACT OR GRANT NUMBER(s): Technical Rpt.
9. PERFORMING ORGANIZATION NAME AND ADDRESS: Naval Underwater Systems Center, Fort Lauderdale Detachment, 1650 SW 39 St., Ft. Lauderdale, FL 33315	10. PROGRAM ELEMENT, PROJECT, TASK AREA & WORK UNIT NUMBERS: A71400, F61512, 36
11. CONTROLLING OFFICE NAME AND ADDRESS: Naval Underwater Systems Center, New London Laboratory, New London, Connecticut 06320	12. REPORT DATE: 29 April 1981
	13. NUMBER OF PAGES: 32
14. MONITORING AGENCY NAME & ADDRESS (if different from Controlling Office): NUSC-TR-6369	15. SECURITY CLASS. (of this report): UNCLASSIFIED
	15a. DECLASSIFICATION/DOWNGRADING SCHEDULE:

16. DISTRIBUTION STATEMENT (of this Report)

Approved for public release; distribution unlimited.

17. DISTRIBUTION STATEMENT (of the abstract entered in Block 20, if different from Report)

18. SUPPLEMENTARY NOTES

19. KEY WORDS (Continue on reverse side if necessary and identify by block number)

Towable sound source
Low frequency transducer
Moving coil transducer
Acoustic target

20. ABSTRACT (Continue on reverse side if necessary and identify by block number)

A towable, low frequency sound source that employs a moving-coil transducer is described. The unit, which consists of a surplus torpedo hull and a specially designed low frequency, broadband transducer, was designed and developed at NUSC's Ft. Lauderdale Detachment. Innovations over previous moving-coil units include design improvements for better heat dissipation, increased moving-coil copper density, more rugged construction, and a stiffer laminated stainless steel and epoxy piston dome. The complete unit is the largest of its kind and produces sound pressure levels in the order of 180 dB//uPa in the 10 to 1000 Hz

DD FORM 1 JAN 73 1473 EDITION OF 1 NOV 65 IS OBSOLETE
S/N 0102-014-6601

20. (Cont'd)

frequency region.

Table of Contents

Page

List of Illustrations ii
Introduction 1
Background and Theory 3
Other Moving-Coil Projectors 3
Failure Analysis 5
Tow Body Considerations 8
The Improved Design 8
- Tow Body 8
- Magnet 8
- Piston 12
- Coil 12
- Seals 12
- Shaft 13
- Springs 13
- Cooling 13
- Compliance Chamber 13
- Air Compensation System 13

Predicted Performance 13
Measured Performance 14
- Transmitted Current Response 14
- Maximum Acoustic Output 14
- Depth Sensitivity 14
- Directivity 17

Conclusions 17
Future Plans 20
Bibliography 21
Appendix A — Equations Describing Moving-Coil Transducer Operation A-1
Appendix B — Effect of Scaling Up Transducer Dimensions B-1
Appendix C — Glossary of Symbols C-1

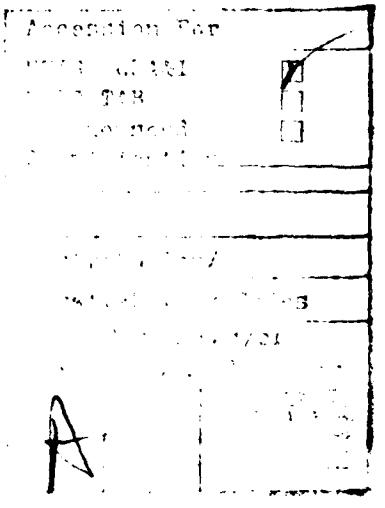

List of Illustrations

Figure		Page
1	Basic Moving-Coil Transducer Construction and Response	4
2	The Effect of Power and Displacement on Source Output	5
3	MRI 216 Transducer Construction and Response	6
4	J-13/15 Transducer Construction and Response	7
5	J-15-3 and MRI 216 Transducer in Tow Bodies	9
6	SEAHORSE Tow Body	10
7	SEAHORSE Transducer Construction	11
8	Comparative Transmitting Current Response, Measured and Theoretical	15
9	XU-1702A Transmitting Current Response	15
10	Maximum Acoustic Output, Several Projectors	16
11	Dual-Transducer SEAHORSE Acoustic Output Level Compared With Several Other Projectors	16
12	Depth Sensitivity, 10 Ampere Drive Level, XU-1702H	17
13	Directivity Index, XU-1702 Single Transducer In Tow Body, at 600, 800, and 1000 Hz	18
14	Single-Transducer SEAHORSE	19
15	Dual-Transducer SEAHORSE	19

A TOWABLE, MOVING-COIL ACOUSTIC TARGET FOR LOW FREQUENCY ARRAY CALIBRATION

Introduction

A continuing trend in the development of the Navy's surveillance and tactical sonar systems is the ever increasing effort to achieve lower frequency detection capabilities. Low frequency arrays can receive plane waves from targets at great distances. Moreover, ambient noise, shipping noise, and self-noise are at higher levels at the lower frequencies.

As a result, one of the problems associated with the development of low frequency arrays is providing calibrated acoustic targets that can generate enough power to overcome the increased ambient noise and the losses associated with distance. These targets are neccessary to measure the effectiveness of present and developmental beamforming and other signal processing techniques. Since most wide aperture arrays have broadband capabilities, the target should also have a broadband capability.

Presently there are no high powered sound sources that have low frequency as well as broadband capabilites. It is possible to connect several units together within a single tow body, but to cover a 10 to 100 Hz band with an adequate amount of acoustic power requires an array of transducers that is prohibitively massive and expensive.

This problem is familiar to the Central Test and Evaluation Activity (CTEA) in Fort Lauderdale, FL, which is tasked with the Test and Evaluation of the Navy's operational, developmental, and experimental towed sonar arrays. During the past 10 years, adequate target generation was provided by the YELLOWBIRD source, a Marine Resources Incorporated tow body and transducer; a J-15-3, a Naval Reseach Laboratory (NRL) transducer array in a tow body; and various ceramic transducers incorporated into another tow body. Until recently, these sources were adequate, if not totally reliable.

Two years ago, the question of how to meet future needs was considered. The basic requirement was for a unit capable of a source level in the order of 185 dB//μPa (at a distance of 1 meter) in the frequency range from 10 to 10,000 Hz. Since the existing ceramic transducers could cover 200 to 10,000 Hz with good reliability in a fairly small package, and could be easily adapted to almost any tow body, the requirements were eased to 10 to 200 Hz, or roughly 4 to 5 octaves.

State-of-the-art transducer design in reasonably large sizes (2 tons or less) was limited with respect to the requirement as follows:

Magnetostrictive — severely displacement-limited, not for low frequencies

Piezoelectric — enormous size below 50 Hz, narrow operating band

Hydraulic — 2 to 3 octave operating band

Electrodynamic — (moving coil) 175 dB//μPa limit, only above 20 Hz (existing half-ton unit).

The investigation also indicated that single magnetostrictive, piezoelectric, and hydraulic units had been built in 2 ton proportions, whereas the largest moving-coil unit was only a half-ton. Two questions immediately arose. Why not combine several moving-coil units for increased output, or why not build a larger moving-coil unit?

To answer the first question, as many as nine moving-coil transducers had been combined into a single array, and the theoretical 6 dB increase in power output for each doubling of the number of transducers had occurred. However, the array is quite massive, does not lend itself to a streamlined tow body, and the low frequency cutoff remains unchanged.

To answer the second question, it is generally accepted, and shown in appendix B of this document, that doubling the mass of a single transducer by scaling its size does not produce a 6 dB increase in power output.

The investigation discussed above still did not indicate abandonment of the moving-coil transducer; so further investigations were conducted. The following additional reasons for abandoning the transducer were offered: historically, moving-coil transducers have been notoriously delicate for at-sea use, they have had inherent depth sensitivity, and they often require a depth compensation device that requires periodic recharging for use at standard operating depths.

Having had some experience with moving-coil sources, the author studied the problems and realized several truths, a fallacy, and possible rectifications of the problems.

By design, a moving-coil transducer is indeed delicate. To achieve optimum performance, it is necessary to minimize the piston mass, and to achieve this, designers use structures that are calculated to withstand the dynamic forces of transducer operation only.

Depth sensitivity comes in several forms; it is primarily a result of the need for the air in the transducer to pass back and forth between two chambers via an air passage whose dimensions can be somewhat limited. The air passage has some flow resistance, which causes damping. As the external hydrostatic pressure is increased, the depth compensation system equalizes the internal air prressure, keeping a minimal differential pressure between the inside and outside of the transducer. As the pressure of the internal air increases, so does its density. This causes increased flow resistance (damping) in the air passage. As a result, transducer output is reduced across most of the frequency band.

The air passage often has a resonance frequency that also affects source output. As pressure increases, the effect of this resonance upon flatness of the source frequency response also increases. The fundamental resonance frequency of the transducer is also a partial function of air pressure. As the pressure increases, the fundamental resonance also increases; however, this effect can be ignored it the transducer is designed to operate above the resonance frequency occurring at the greatest depth.

The third disadvantage of moving-coil transducers was reported to be that of air consumptiom, which can occur in three different ways. First, when the source is lowered to operating depth, air from the high pressure storage tank is released into the transducer; when the source is retrieved, the air is exhausted. This is unavoidable in all but the most complex regulation systems, but it does not limit the time at operating depth. Second, air can be expended during the normal small depth excursions that occur because of changes in tow speed or bobbing of the tow ship. However, most compensation systems contain an accumulator which can recycle the air for depth changes up to 100 percent depending upon the relative volumes of the accumulator and the compliance chamber, and the maximum operating depth. Third, air can be expended through "pumping" of the regulator by intense, low frequency sound pressure levels. This can be controlled by placement of the regulator in a free-flooding chamber whose flooding holes provide sufficient viscous damping to restrict the alternating flow of sea water. The YELLOWBIRD had such a system and was operated continuously for 10 days during one tow with no air expended after initial deployment.

To summarize the situation, it appeared that the most effective way to achieve high level, low frequency, broadband coverage was to improve upon the moving-coil transducer by extending its low end response, increasing its output (possibly by increasing size and heat transfer characteristics), and improving its reliability through more rugged construction.

A brief discussion of moving-coil theory and background will be helpful in understanding the approach finally decided upon.

Background and Theory

Figure 1 shows a typical current response curve. ω_o is the resonance frequency created by the spring-mass system consisting of air and spring compliances and the piston and water mass. Below resonance, motion is stiffness-controlled, and response drops off at -12 dB/octave. Above resonance, the response is mass-controlled, and acoustic output is theoretically flat for a constant current input. The deviation in response at midpoint is typical of the air passage resonance effect, and the high frequency cutoff occurs at a frequency of the first piston face flexure-mode resonance.

Displacement limitation is usually in the form of physical stops, which may or may not be within the operating reach of piston travel.

It is shown in appendix B that scaling up the size of a transducer offers surprisingly few advantages over increasing the number of transducers; however, to fill a given cylindrical space with cylindrical transducers, the use of a single large unit offers an advantage over the use of an array of smaller units by filling the envelope with effective transducer mass. In addition, scaling up transducer dimensions reduces the delicacy of certain components and permits the machining of weight-saving structural design techniques that are impractical in small proportions.

Increasing transducer size not only increases output power, but it also lowers the lowest full power operating frequency by increasing displacement: the piston-area/piston-travel product. The effects of these two changes are shown in figure 2. Also, it is implied in appendix B that the single transducer approach provides a lower maximum power operating frequency than does the multiple unit approach.

Figures 3 and 4 show two existing moving-coil transducers that have been more successful than most. Figure 3 shows the Marine Resources Incorporated MRI 216, which until recently was the largest moving-coil projector in existence. It has a 30 cm (12 in.) diameter piston and a 320 kg (700 lb) magnet. The air passage between the volume under the piston and the compliance chamber is a series of small holes in the piston wall and several holes in the magnet pole piece. Downward travel is limited by the magnet structure and upward motion by the spring retainers. The unit is designed to operate within displacement limits of ± 0.6 cm ($\pm 1/4$ in.). The coil is the same length as the pole piece so that any significant displacement causes a loss of efficiency and linearity. Coil heat is dissipated principally by convection and conduction through the internal air to the magnet. The response curve shows the depth sensitivity in the form of reduced output across the frequency band and in the resonance effect between 80 and 100 Hz.

Figure 4 shows a J-13 transducer (NRL). The response curve is particularly flat out to 3 kHz. The air passage is through the center of the magnet via holes in the bearing holder. Heat is dissipated to the magnet via oil which is contained by the top and bottom rubber seals. The lower seals also act as centering springs. The depth sensitivity characteristic (not available) is in the form of a deviation in the 250 Hz frequency region.

Both configurations have advantages and disadvantages. The oil heat dissipation media in the J-13 permits the use of higher currents than air would allow, but in order to repair any part, the magnet must be demagnetized and completely disassembled. On the other hand, the piston of the MRI 216 can be lifted out easily with little disassembly. The outside air passage of the MRI 216 makes maximum use of the volume available for magnetic material, but the small holes are restrictive and create depth sensitivity across the frequency band. The MRI 216 and J-13 anodized aluminum pistons are light and provide good electrical insulation, but their coefficients of thermal expansion are twice that of copper, causing coil stretching and rubbing against the magnet walls at moderately high temperatures. Both magnets are encased in air-filled chambers. This limits the dissipation of heat, especially in the J-13 where heat flow is relatively unobstructed between the coil and the magnet.

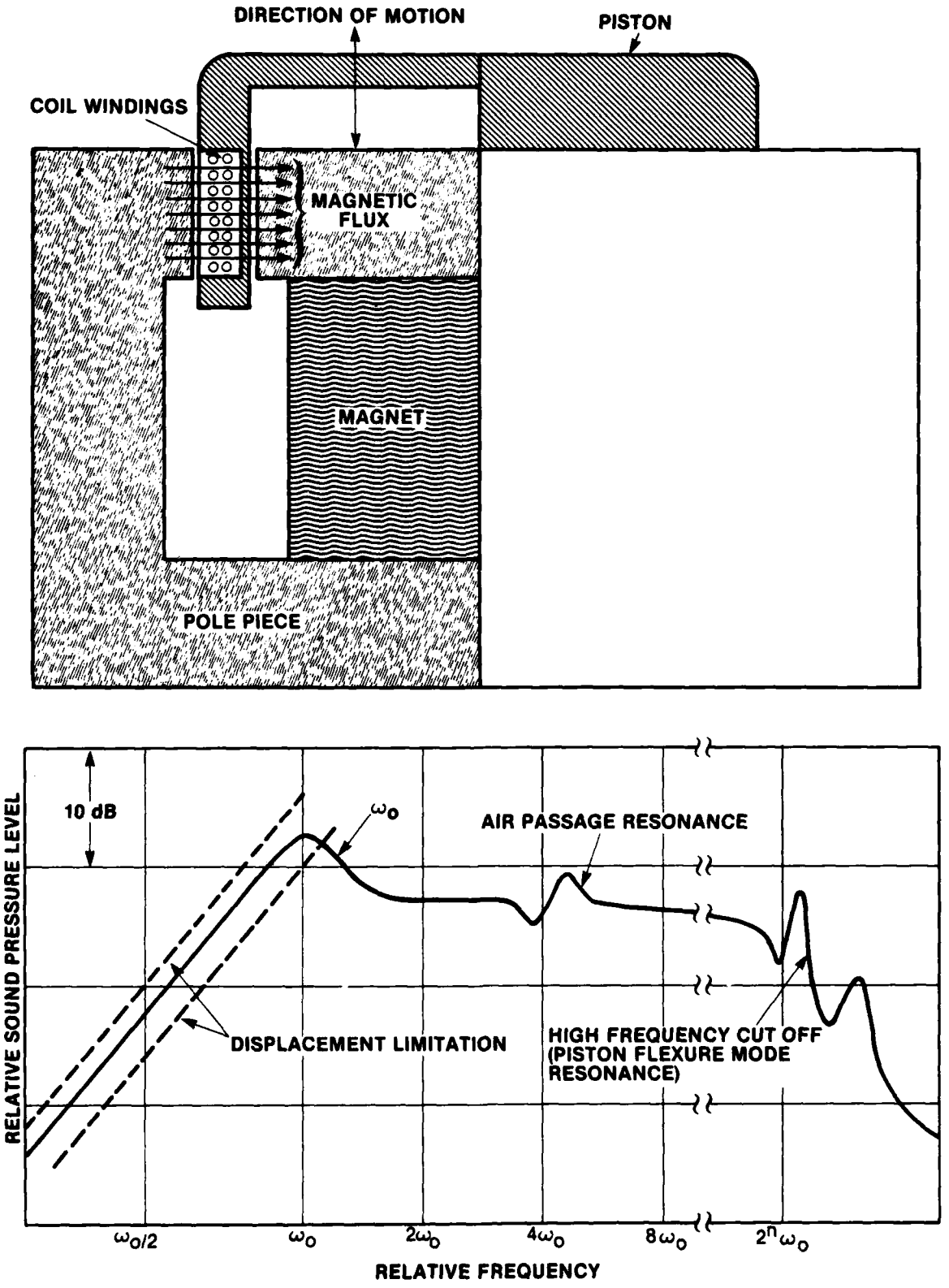

Figure 1. Basic Moving-Coil Transducer Construction and Response

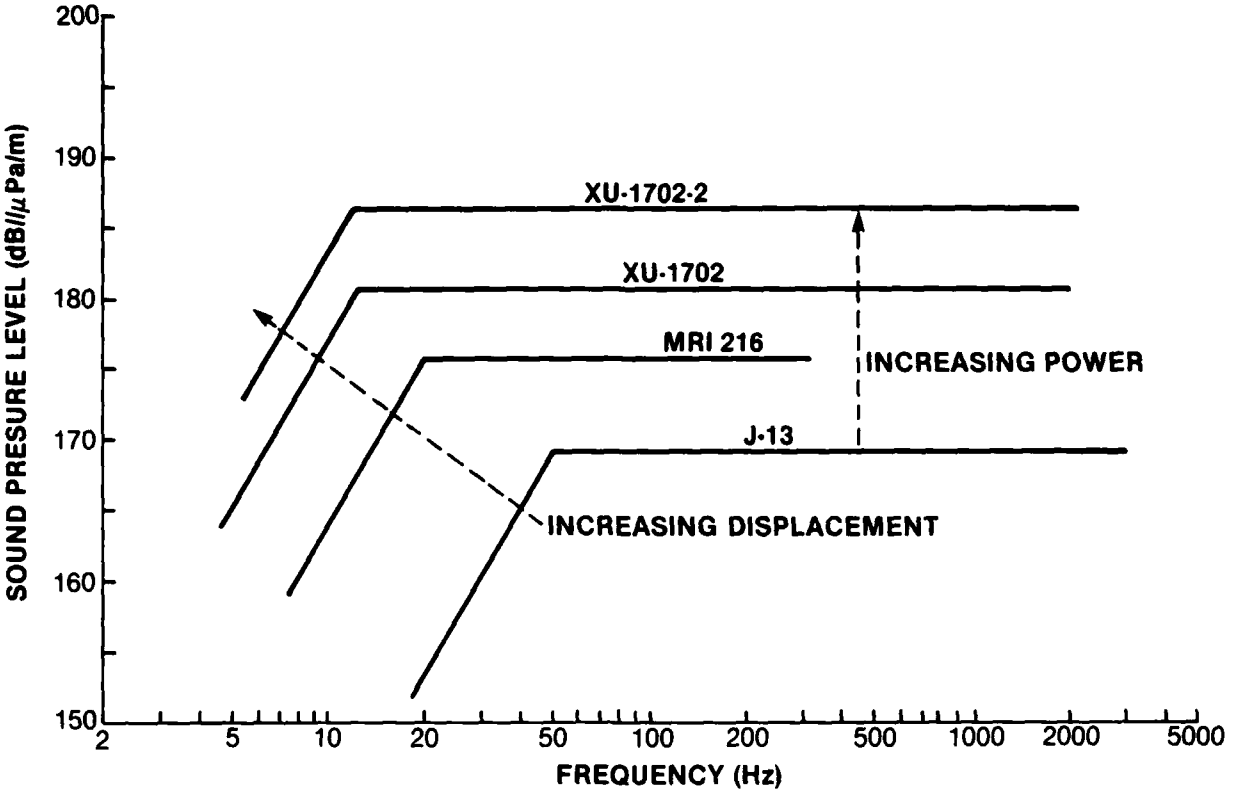

Figure 2. The Effect of Power and Displacement on Source Output

Failure Analysis

An examination of common failure modes of moving-coil transducers will give some insight into more reliable design.

1. *Coil Burn-Out* — The most common causes of failure result from the user exceeding the established operating power limit in an effort to get "just one more dB." The higher current can burn out the coil by exceeding the temperature limit of the bonding material or wire insulation.

2. *Coil Stretch* — Coil form expansion with heat may become excessive, stretching the copper wires.

3. *Coil Abrasion* — Coil form expansion may also cause the coil windings to rub against the outside pole piece, baring the wire and shorting it.

4. *Particles* — Iron or other particles in the magnetic gap may rub against the coil, shorting it out.

5. *Nonconcentricity* — The coil form may often become slightly nonconcentric during handling because of its delicate construction, causing rubbing in the gap.

6. *Piston Skew* — A slight amount of skew in axial piston alignment may cause rubbing against the pole piece.

7. *Power Transients* — Shipboard power transients coupled through the drive amplifier may drive the piston against its stops, shocking and deforming it.

8. *Fast Depth Change* — If operating depth changes too fast for air compensation, the piston may operate off-center, causing it to vibrate against the stops.

9. *Seal Failure* — Fast changes in depth can also cause seal failures because of excessive differential pressure between the transducer interior and exterior.

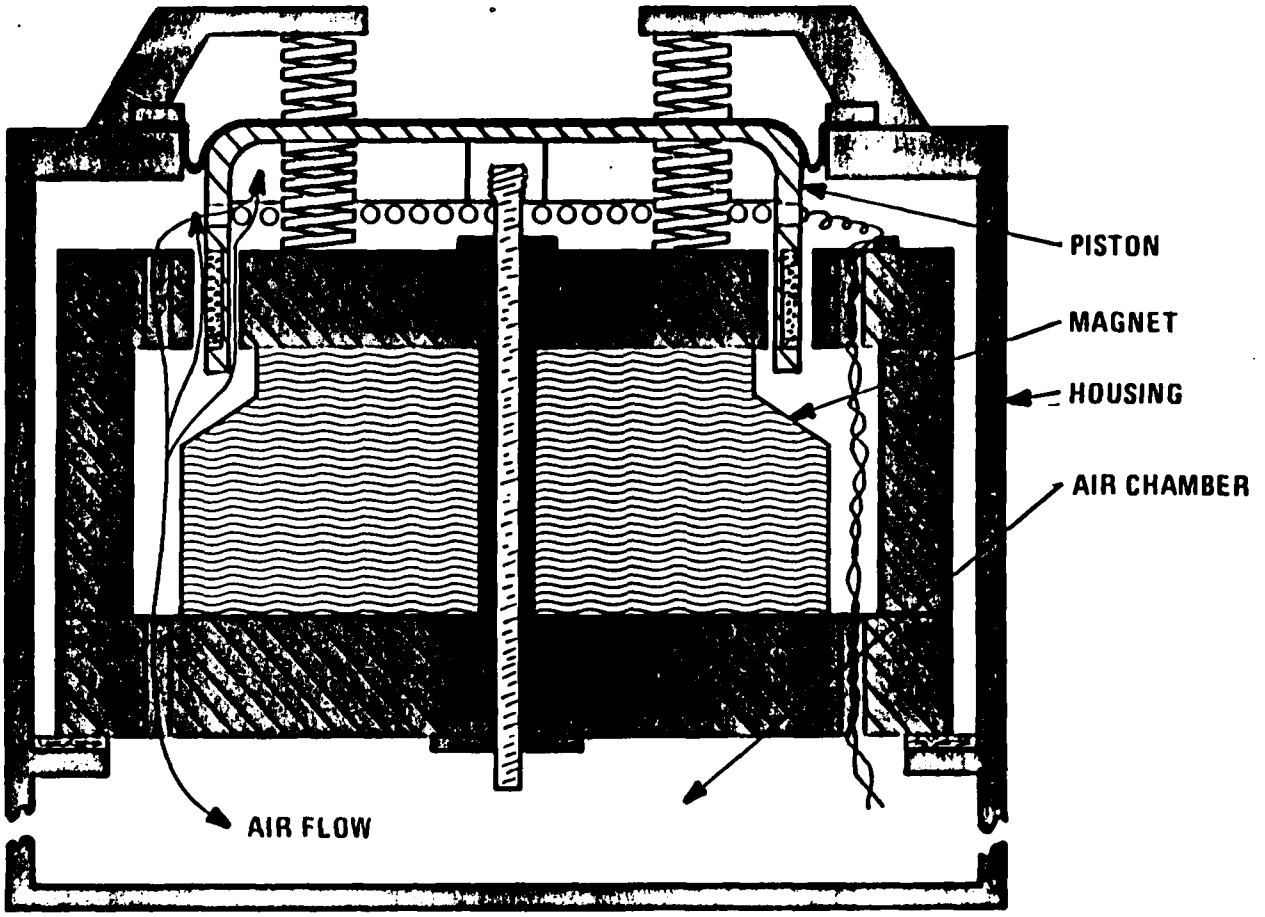

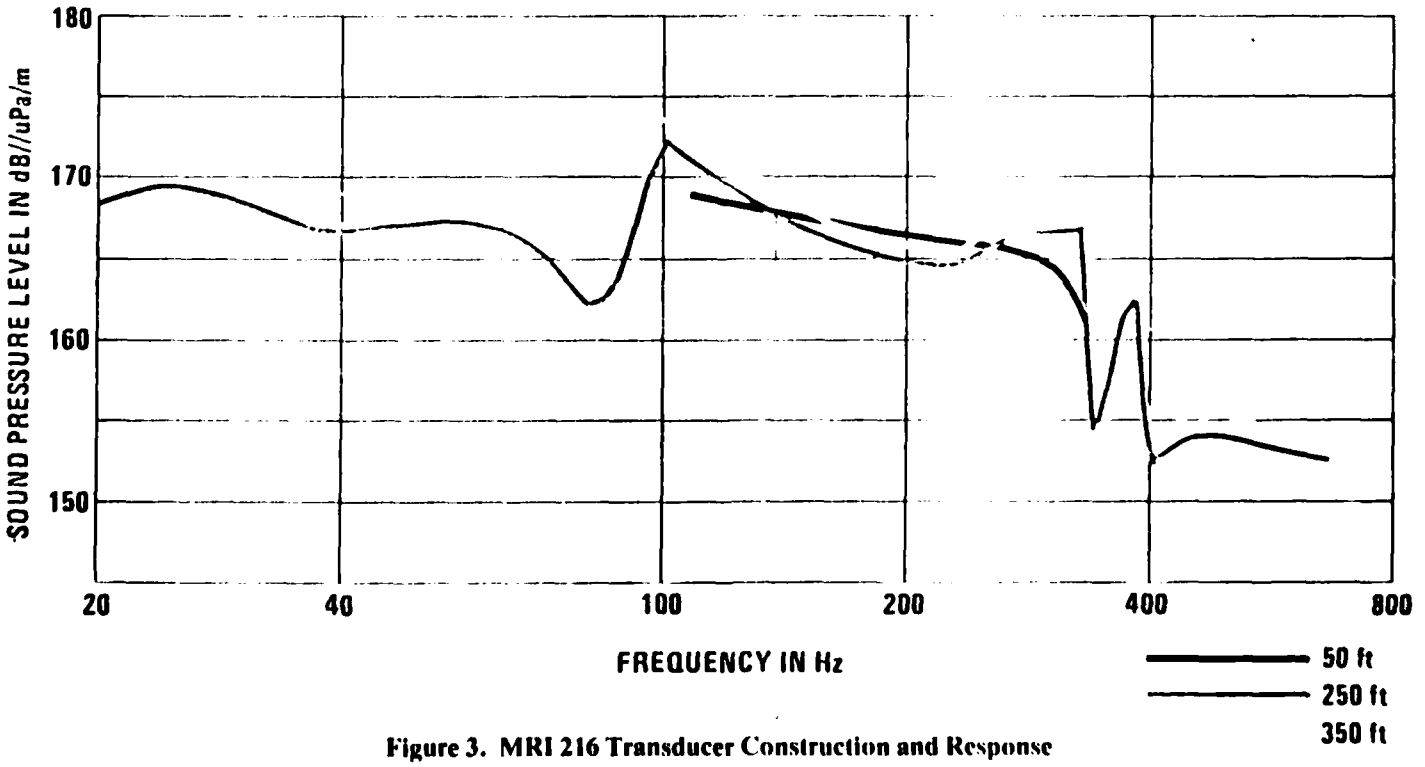

Figure 3. MRI 216 Transducer Construction and Response

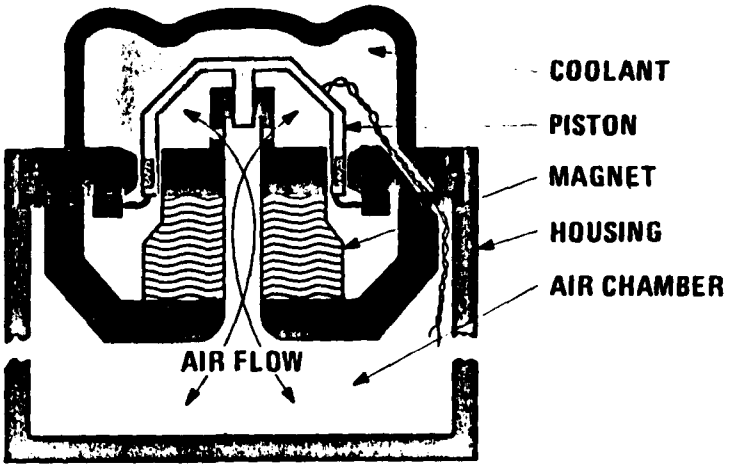

NAVAL RESEARCH LABORATORY J-13/15

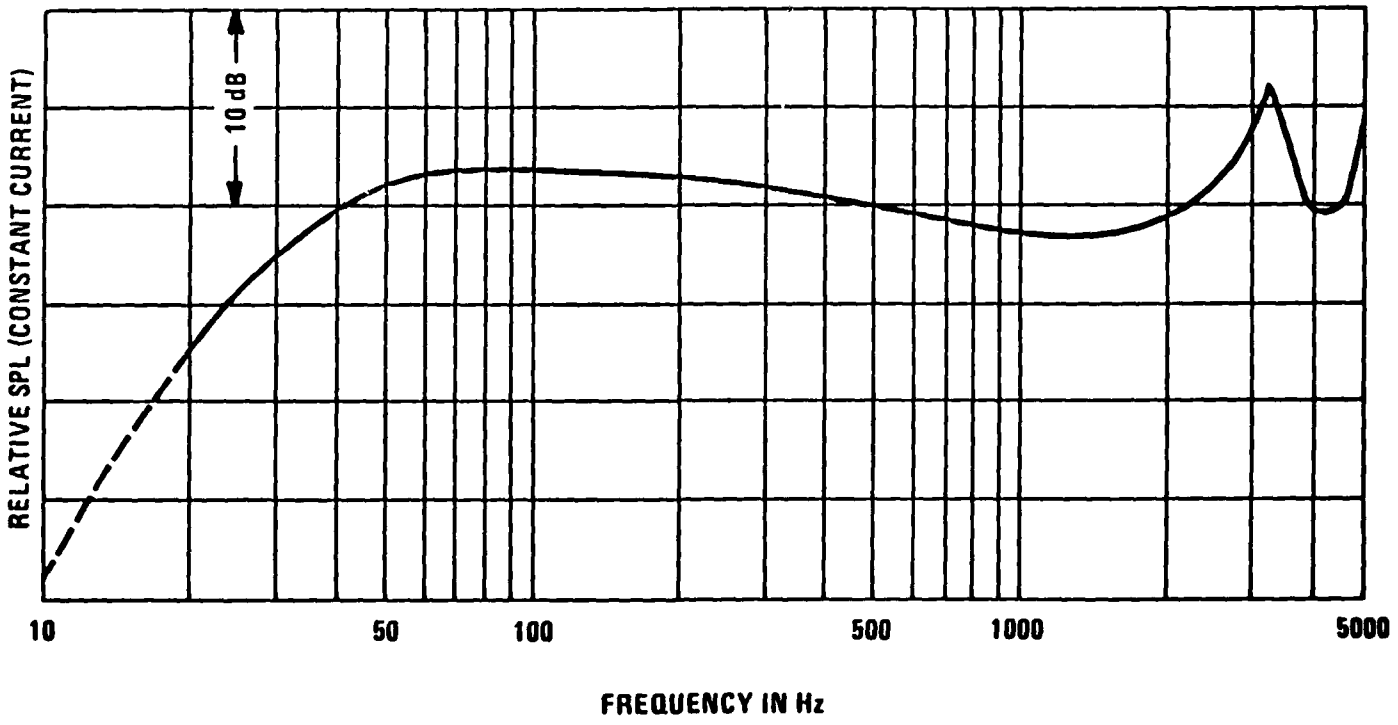

Figure 4. J-13/15 Transducer Construction and Response

10. *Lead Wire Failure* — The lead wires attaching the coil to the transducer housing can fatigue or snap because of excessive piston travel during depth changes.

Tow Body Considerations

Figure 5 shows the tow bodies of the MRI 216 and the J-15-3 (which is essentially three J-13's). While these bodies do serve their intended purpose, they are quite large compared with the transducer. Transducer design that takes into consideration placement in a tow body should improve this situation.

The Improved Design

The final product of the design effort integrates (1) the best features of the MRI 216 and J-13, (2) several previously untried improvements, and (3) tow body design considerations. The design emphasis was on simplicity, rugged construction, and heat dissipation efficiency rather than on power efficiency — the philosophy being that power efficiency is less important than total output. Figures 6 and 7 show the tow body and transducer, each part of which is discussed below.

Tow Body

It probably seems a bit unorthodox to design the tow body first; however, the availability of tow bodies that were ideal in size, shape, strength, and cost (zero) was impossible to ignore. A surplus Mk 41 torpedo hull, 53 cm (21 in.) in diameter, was used as the tow body. The Mk 41 torpedo is especially suitable because of its long tapered tail and large surface-area, shrouded tail fin. The blunt nose has become accepted as a better hydrodynamic design than the older, round nose. This selection fixed the diameter of all major source components.

The long cylindrical tow body determined the transducer configuration. Moving coil transducers are typically cylindrical; however, operation with the axis oriented horizontally requires extra lateral support in the suspension and centering systems to offset the forces of gravity and buoyancy.

The nose of the tow body is filled with lead to keep the center of gravity forward for better towing stability. The acoustic windows are 47 percent open, perforated, stainless steel, allowing an open area that is 3 times the piston area. The magnets and compliance chamber are bolted together and have 0-ring seals. Next in line are the air bag, regulator, and tank chambers.

Magnet

The design of the air passage through the magnet was borrowed from the J-13, but was made disproportionately larger to reduce the resonance effects.

The magnet was configured to have the outer pole piece in intimate contact with the water rather than to have it encapsulated in an air-filled canister. This would greatly improve heat transfer from the coil and pole pieces to the sea water and is consistent with the emphasis on heat dissipation efficiency. The magnet designer was asked to design the magnet with the following constraints/requirements.

1. Outside diameter	—	53 cm (21 in.)
2. Magnet material	—	optimum material for this type of transducer
3. Gap diameter and width	—	optimum flux density-gap volume product
4. Pole piece length	—	5 cm (2 in.)
5. Magnet center hole	—	10 cm (4 in.) diameter
6. Maximum weight	—	450 kg (1000 lb)

The Alnico V-7 magnet material had been selected by the three manufacturers contacted as the most appropriate material. The size of the piston would be determined by the magnet designer's optimum gap diameter and width. Total weight was 340 kg (750 lb).

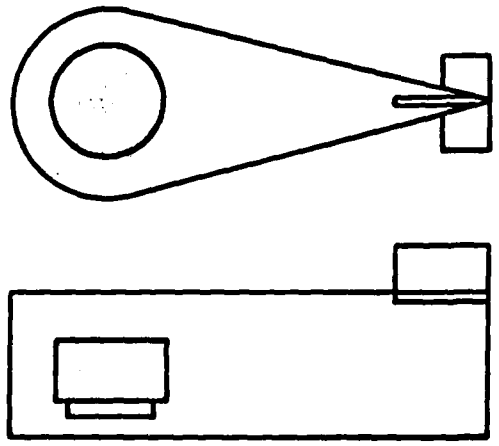

J-15-3 TOW BODY

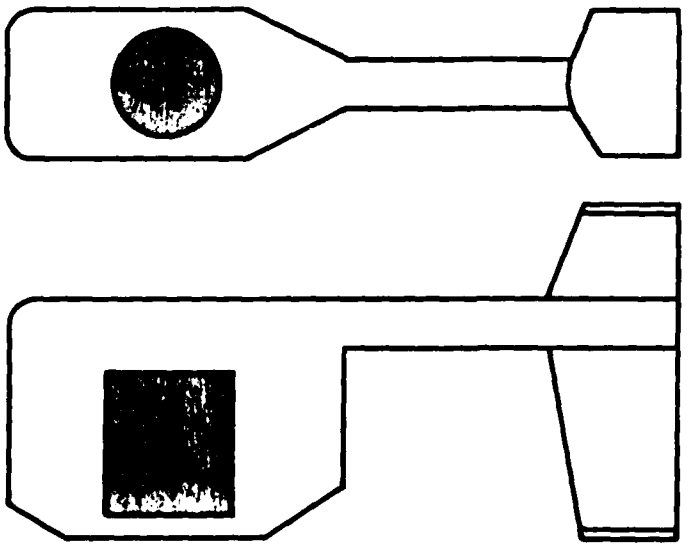

MRI-216 TOW BODY

Figure 5. J-15-3 and MRI 216 Transducer in Tow Bodies

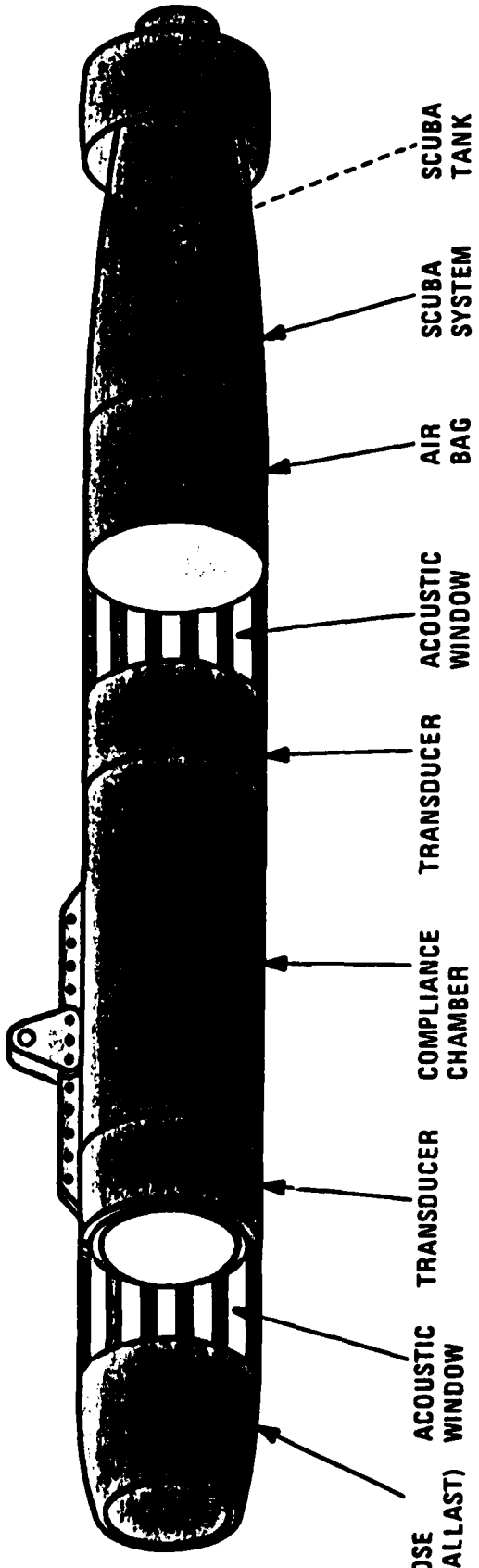

Figure 6. SEAHORSE Tow Body

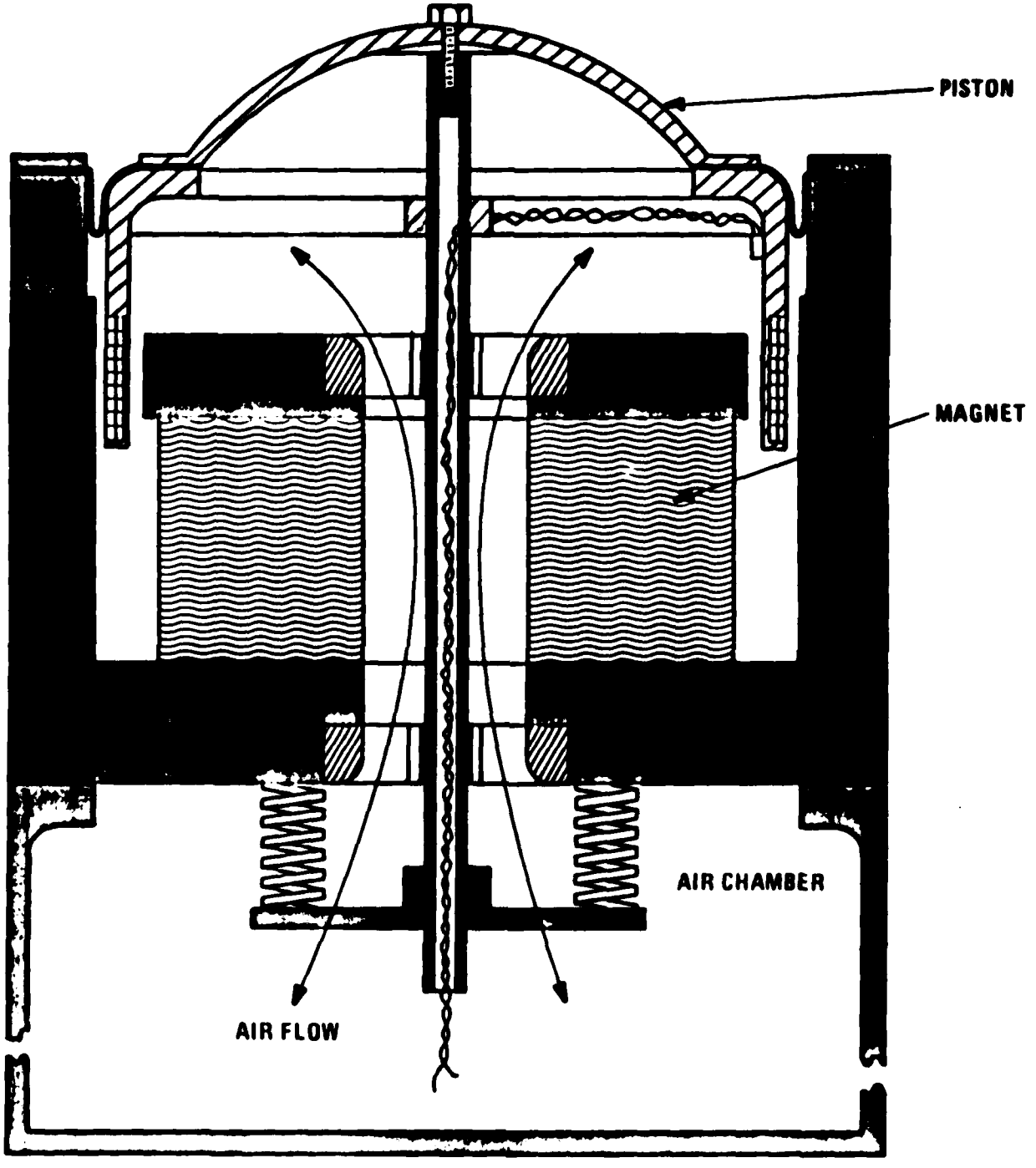

Figure 7. SEAHORSE Transducer Construction

The design produced a 40 cm (16 in.) diameter gap which was 0.6 cm (0.250 in.) wide. The final flux density was 0.9 weber per square meter (9000 gauss), which was 90 percent of the predicted value. The Alnico V-7 process limited the design length of the magnet; therefore, the full 450 kg (1000 lb) maximum weight was not reached. A serious time delay occurred because of the scarcity and rapidly rising cost of cobalt on the world market. Cobalt is an essential ingredient in the manufacture of all Alnico, but an especially high percentage is used in Alnico V-7. All iron magnet surfaces were nickel plated.

Piston

If the piston was to be less than 50 cm (20 in.) in diameter, then to produce 185 dB//μPa at 10 Hz would require at least a 10 cm (4 in.) piston stroke. This seemed a bit risky at a time when 1 cm strokes were maximum, so that the use of two transducers, in-line and back-to-back, was decided upon. This would add only a little more drag to the tow body and would reduce the stroke requirement down to approximately 5 cm, still unprecedented, but not as risky. The use of long strokes requires that the pole piece and coil be different lengths. To provide perfectly linear motion, the difference would have to be the same as the stroke, or 5 cm. To keep the magnet dimensions fairly small, a 5 cm pole piece and a 7.5 cm coil length were decided upon. This would allow for linear motion for a 2.5 cm stroke, or 185 dB μPa at 16 Hz. To produce the same level at 10 Hz, some harmonic distortion would occur since the coil would have only 66 percent of its windings in the magnetic gap. Setting the resonance at 10 Hz would minimize the loss in linearity and efficiency. The back-to-back placement of the transducers also would negate tow body vibration.

The magnetic gap dimensions fixed the piston diameter at 40 cm (16 in.) with a wall thickness of 530 mm (0.210 in.). Berylium copper was chosen as the coil form material for its thermal coefficient of expansion, which is close to that of copper. Berylium copper was also a good choice for heat dissipation as it would distribute the coil heat along its surface, effectively increasing the heat dissipation area. The piston face was made of two layers of stainless steel spun into a conical shape and sandwiched together with epoxy. A two-point shaft attachment was used to reduce piston skewing. This was felt to be essential because of horizontal operation. The piston was designed to allow the coil lead wires to be routed through the hollow centering shaft and plastic tubing to the compliance chamber wall. This proved very successful in eliminating wire fatigue and failure.

Coil

The coil was also designed with emphasis on heat transfer. Instead of using conventional small, round cross-section wire; large, square cross-section wire was used. The benefits were threefold:

1. Square wire would increase the copper density of the coil by reducing the amount of fill-in bonding material, thereby permitting higher coil current density at the same temperature.

2. Internal heat in the coil could more easily be conducted to the exterior surfaces through the increased copper.

3. The use of large wire also increased the copper density as a higher copper-to-insulation ratio resulted.

The resulting low impedance coil, approximately 1 ohm dc resistance, required high current, low voltage operation. This would reduce the number of high voltage breakdowns which normally occur in underwater transducers, but would require larger tow-cable conductors.

A temperature sensor was embedded in the hottest part of the coil to set and monitor operational temperatures to prevent coil burnout.

Seals

The seals are conventional rubber rolling seals, the same type used in the MRI 216. Since

there was not enough lead time to have seals manufactured to specifications prior to the first use, the closest commercially available shape, half of an inner tube, was used. Since the differential pressure across the seal cannot exceed 1 psi because of the SCUBA system exhaust check valve, there was little danger of a blowout.

Shaft

The bronze bushings are supported by bearing holders that incorporate the flared passage openings. The shafts, per specification of the bearing manufacturer, are 80 case-hardened stainless steel, chrome plated and centerless, ground to ±.0026 mm (±.0001 in.) in precision.

Springs

The springs used for this application had a total stiffness that produced a transducer resonance frequency of 14 Hz.

Cooling

The transducer can be operated with air or fluid cooling between the coil and the magnet pole piece. Both cooling media have been tried and the results are reported in the "Measured Performance" section.

Compliance Chamber

The compliance chamber was designed to be open to both transducers, giving a resonance frequency of 14 Hz at an internal pressure equivalent to a depth of 90 m (300 ft). The combined air and spring components produce a resonance frequency of 20 Hz at a depth of 90 m.

Air Compensation System

The air system consists of a cone-shaped air tank which fits perfectly into the tail section of a Mk 41 torpedo, a spherical air bag, and a standard two-stage SCUBA regulator. The air bag compensates for small changes in depth without expending air. With this system, no air is expended during towing if the depth is maintained within ±10%, which is easily accomplished with faired cable. To solve the problem of air expenditure due to regulator cycling by sound pressure levels at low frequencies, the regulator is located in a free-flooding chamber in the tail section. The flooding holes provide enough viscous fluid damping to substantially restrict dynamic sound pressure.

Predicted Performance

Performance predictions computed for this unit are of the most basic form. Taking into account all of the internal losses due to friction, viscous damping, eddy currents, flexural vibration modes, etc., was considered pointless since such computations are quite time-consuming and seldom accurate.

The calculation of displacement-limited operation and idealized transmitting current response (TCR) is straightforward. The interesting quantity will be the total losses, or the difference between the theoretical TCR and the measured value.

Displacement limited output is defined by

$$p_{max} = \omega^2 \varrho_o a^2 \xi_{max} / 4r \ ,$$

where

p_{max} = sound pressure level
ω = angular frequency
ϱ_o = density of water
a = piston radius
ξ_{max} = piston travel limit
r = distance from transducer.

It is evident that displacement-limited output pressure increases with ω^2, or at a rate of 12 dB/octave.

The design displacement of the transducer is set by the coil, which is 7.5 cm (3 in.) long, and the magnet gap, which is 5 cm (2 in.) long, allowing for a total displacement of 2.5 cm (1 in.) peak-to-peak for undistorted output.

For the SEAHORSE (single transducer),

p = 183 dB//μPa/m at 20 Hz

and

p_{max} = 171 dB//μPa/m at 10 Hz.

For the MRI 216 (assuming a 1.25 cm (1/2 in.)) peak-to-peak displacement,

p_{max} = 172 dB//μPa/m at 20 Hz

p_{max} = 160 dB//μPa/m at 10 Hz.

For the J-13 (assuming a 1.25 cm (1/2 in.)) peak-to-peak displacement,

p_{max} = 164 dB//μPa/m at 40 Hz

p_{max} = 152 dB//μPa/m at 20 Hz.

The TCR is defined by

$$p_{tcr} = F\varrho_o a^2/4M_t r \ ,$$

where

F = force = B*l*i
M = total mass
r = a distance of 1 meter
B = flux density
l = length of coil wire
i = 1 amp.

For the SEAHORSE,

p_{tcr} = 149 dB//μPa.

For the MRI 216,

p_{tcr} = 160 dB//μPa.

For the J-13,

p_{tcr} = 165 dB//μPa.

Maximum power output is determined by the rate of heat dissipation from the coil and the maximum allowable operating temperature of the coil. This quantity is normally determined experimentally since heat dissipation due to conduction, radiation, and convection is very difficult to predict.

Measured Performance

Transmitted Current Response

Figure 8 shows the measured and predicted TCR's for the SEAHORSE (XU-1702) transducer as well as for the MRI 216 and the J-13. This particular SEAHORSE transducer was designed to resonate at a frequency of 13 Hz at a depth of 15 m (50 ft). This configuration included a 1 m (40 in.) long compliance chamber; a 0.5 m (20 in.) long chamber would resonate at 17 Hz, a 2 m (80 in.) chamber at 11 Hz. The means to calculate these predictions are given in appendix A.

Figure 9 shows the response of a SEAHORSE transducer that employed a 1.2 m (48 in.) compliance chamber. The TCR is 6 dB higher because the coil consisted of four layers of smaller wire, resulting in twice as many turns. The TCR is less uniform, because a thin experimental piston dome was used. The figure shows the lower resonance frequency attributed to compliance chamber length.

Maximum Acoustic Output

Figure 10 shows the maximum sound pressure levels attainable by the three projectors. The SEAHORSE level is based upon a 50 ampere (34 dBa) current drive level. This drive level has been maintained for 2 hours in tests run at NRL's Leesburg, FL, facility.

The SEAHORSE has been operated with two transducers back-to-back as originally conceived. Levels were 6 ± 1 dB higher than for the single unit. Work is in progress to improve heat dissipation by filling the air gap between the coil and the magnet with thermally conductive fluid. The most promising fluid appears to be *ferrofluid*, which is a colloidal suspension of iron in an ester base. The presence of iron causes the fluid to remain in the gap area, precluding the need for seals. Preliminary measurements show that the transducer can be operated at the 70 ampere (27 dBa) drive level while maintaining coil temperature below 100°C. The present 50 ampere drive level creates operating temperatures of 200° C.

Figure 11 shows the ultimate capability of a fluid-cooled, two-transducer SEAHORSE. Included in the figure are maximum sound pressure characteristics of several other projectors currently in use.

Depth Sensitivity

Figure 12 shows the depth sensitivity down to 45 m (150 ft) for the most recent single-

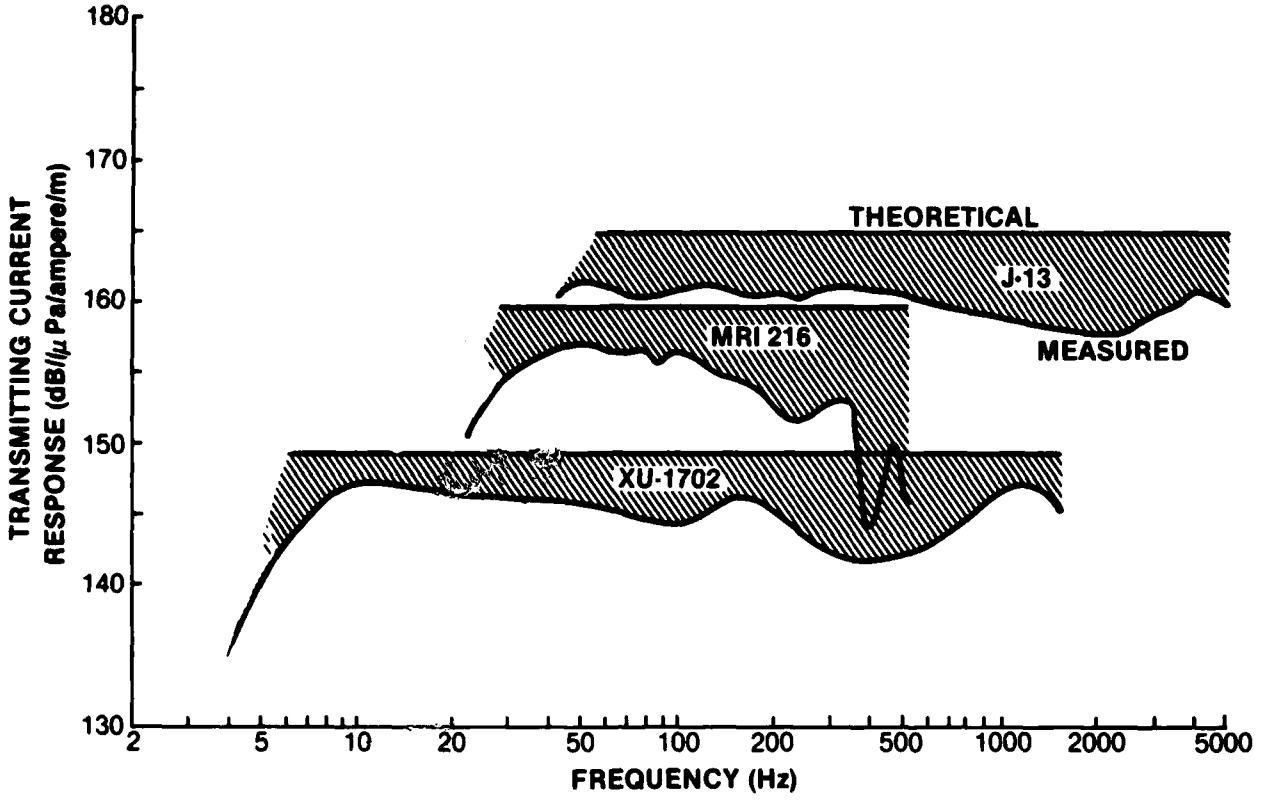

Figure 8. Comparative Transmitting Current Response, Measured and Theoretical

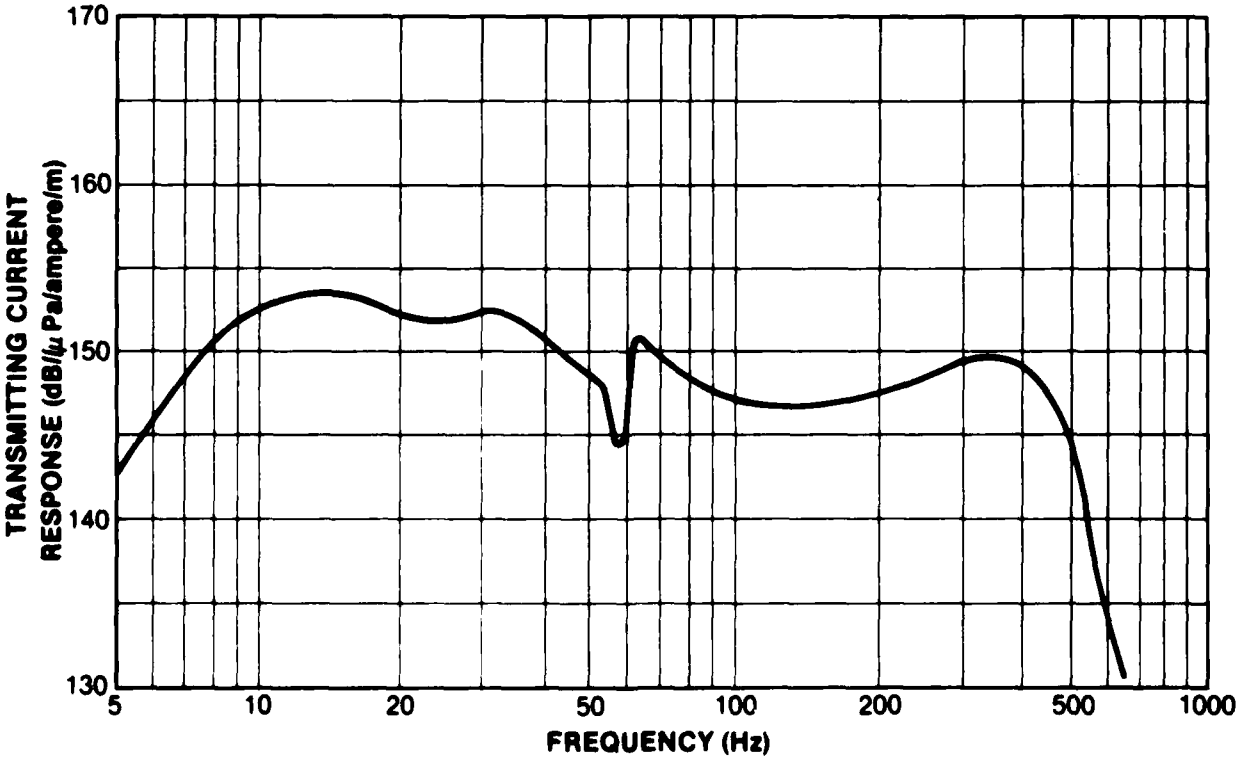

Figure 9. XU-1702A Transmitting Current Response

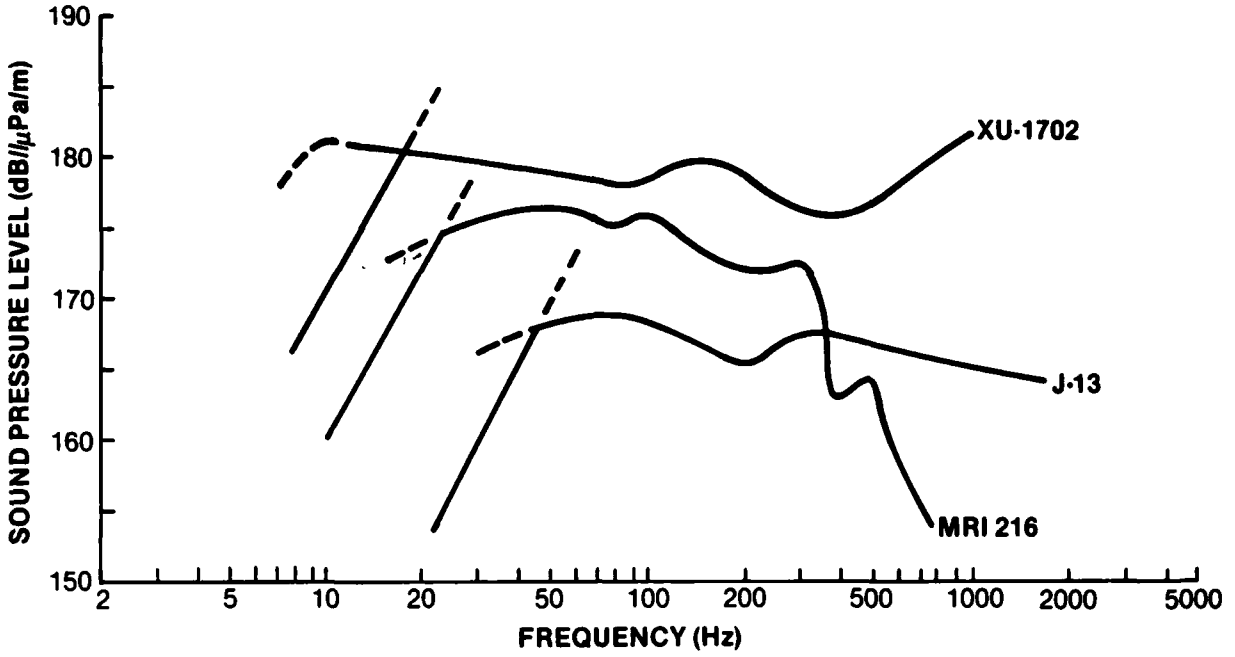

Figure 10. Maximum Acoustic Output, Several Projectors

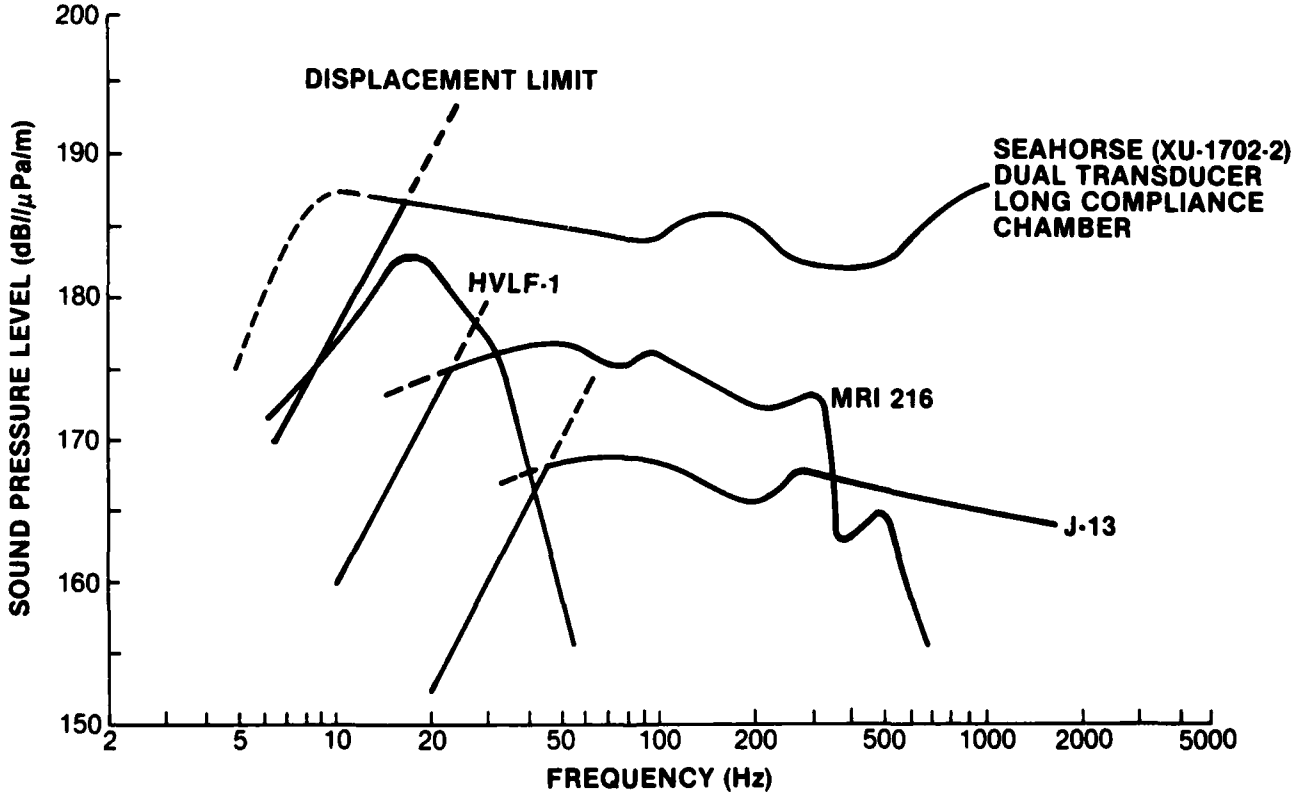

Figure 11. Dual-Transducer SEAHORSE Acoustic Output Level Compared With Several Other Projectors

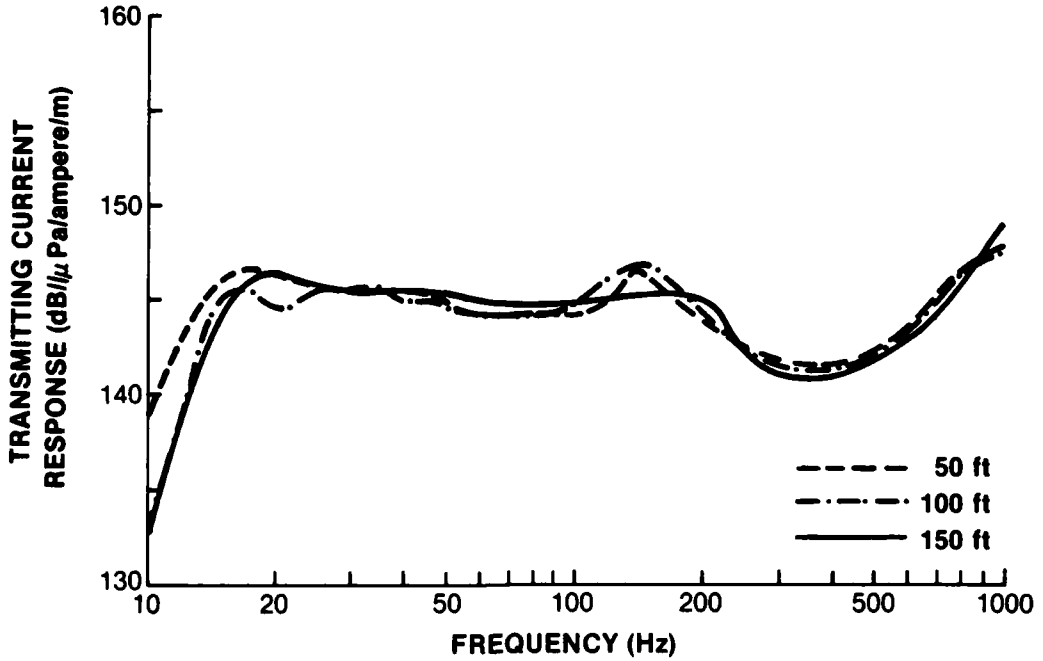

Figure 12. Depth Sensitivity, 20 Ampere Drive Level, XU-1702H

transducer XU-1702H. The 17 Hz resonance occurring at 15 m (50 ft) is predictable; however, prediction also shows 26 Hz resonance 15 30 m (100 ft), and 31 Hz resonance at 45 m (150 ft). The 30 m (100 ft) curve indicates the presence of a second low frequency resonance which may have shifted slightly in the 45 m characteristic. Suspect is the air bag and its coupling to the compliance chamber and the water. This phenomenon will be examined during FY81.

Even more interesting is the absence of a mid-band response deviation, characteristic of the resonant air passage effect in the MRI 216 and J-13.

Directivity

Figure 13 shows the high frequency directivity of a single-transducer SEAHORSE. The unit,shown in figure 14, is omnidirectional up to 600 Hz. The dual transducer unit is shown in figure 15.

Conclusions

1. Compared with its predecessor, the "YELLOWBIRD" (MRI 216), the SEAHORSE (single-transducer version) is 226.8 kg (500 lb) lighter, output is doubled, tow body cross-sectional area (normal to flow) is halved, and length is the same.

2. The improved coil design using square wire and a berylium coil form has improved the SEAHORSE power-handling capability.

3. Placement of the magnet pole pieces in direct contact with the sea water has also improved heat dissipation.

4. The sandwich construction used in the dome has resulted in a lightened, stiffer dome which reduces total mass and extends high frequency response.

5. The large air passage has eliminated mid-band resonance anomalies.

6. The integration of transducer and tow body designs has resulted in a source having superior towing characteristics.

7. Rugged construction, although costly in piston mass, has paid off in improved reliability.

8. Also aiding reliability is the inclusion of temperature sensors imbedded in the moving coil, allowing continuous monitoring of the coil thermal condition.

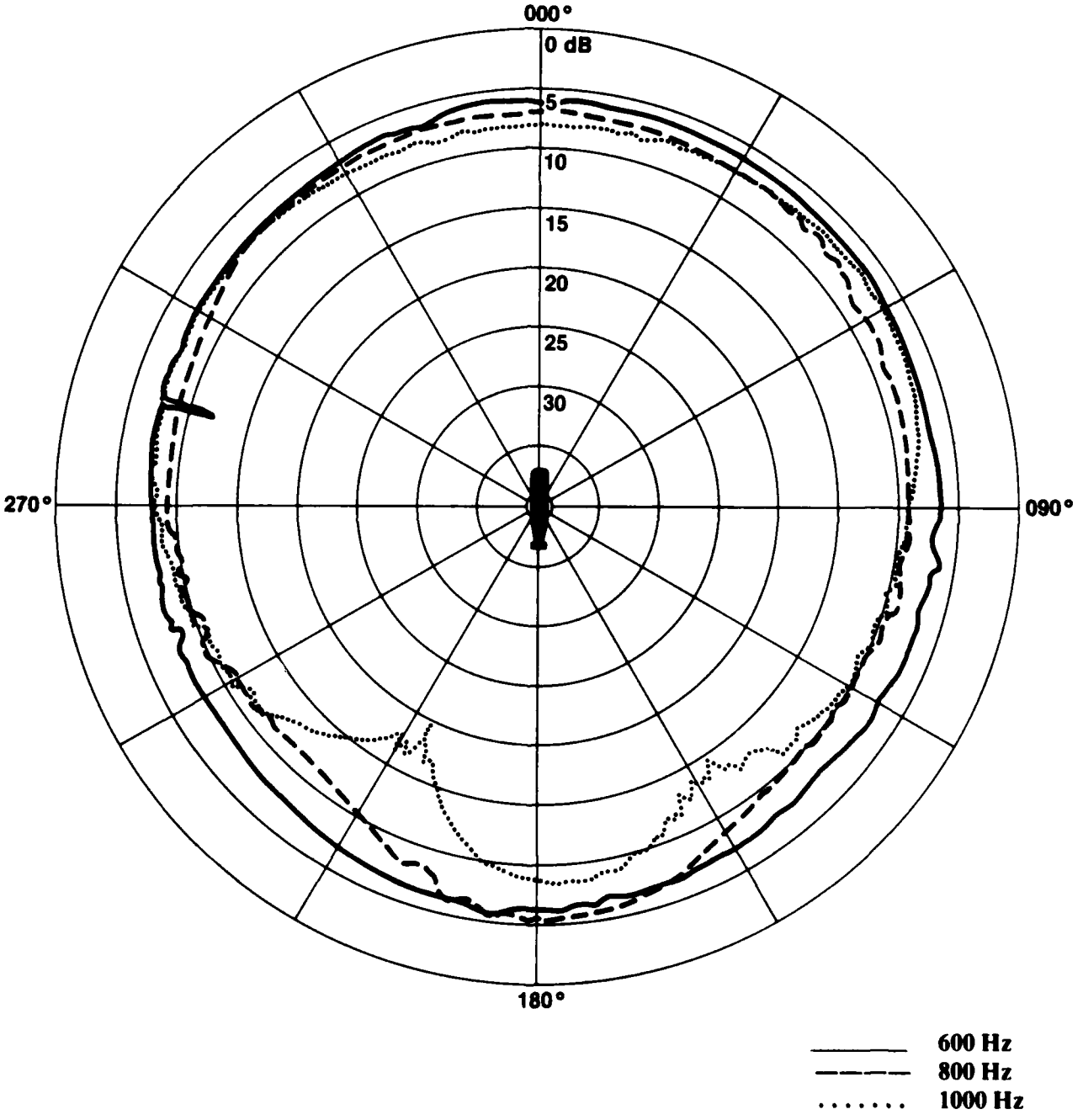

Figure 13. Directivity Index, XU-1702 Single Transducer In Tow Body, at 600, 800, and 1000 Hz

Figure 14. Single-Transducer SEAHORSE

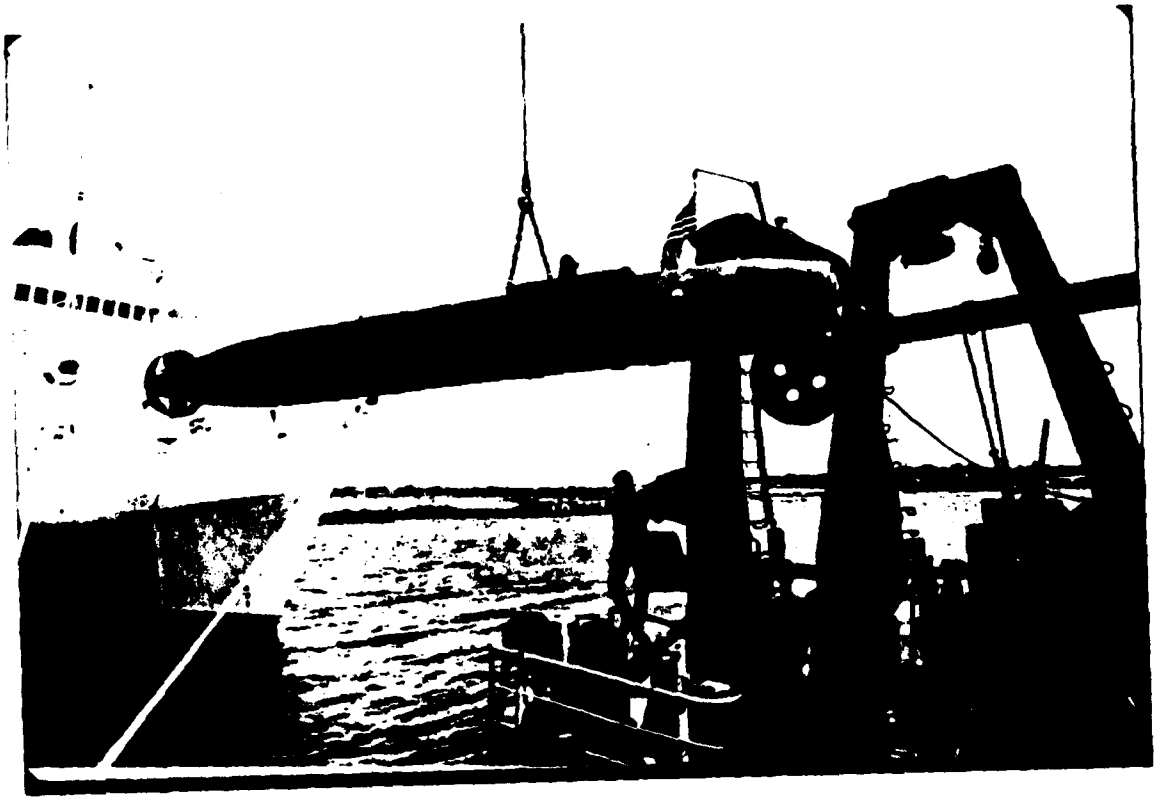

Figure 15. Dual-Transducer SEAHORSE

Future Plans

NUSC's Fort Lauderdale detachment houses an ongoing moving-coil transducer development program, motivated largely by the results of SEAHORSE development. During FY81, effort will be applied in the following areas:

1. Composite materials (boron-tungsten-epoxy, graphite/epxoy, etc.) to lighten and strengthen transducer moving components

2. Rare earth-cobalt magnet materials, which offer 4 to 5 times the energy product of the best Alnico magnets

3. Ferrofluid cooling, already mentioned, which should significantly improve heat dissipation capability

4. Flat, teflon coated wire, which will increase coil electrical impedance for lower drive currents, improve radial heat dissipation efficiency, and boost coil copper density

5. Restructuring the traditional transducer configuration for resonance-free, low mass, high breakup frequency, and highly reliable operation

6. Study and implementation of techniques that will reduce inefficiency due to eddy currents generated within the iron pole pieces.

Bibliography

Bobber, R. J., "Underwater Acoustic Measurements," Library of Congress Catalog Card No. 72-608304, July 1970

Groves, Jr., I. D., "Twenty Years of Underwater Electroacoustic Standards," NRL Report 7735, 21 February 1974.

Hugus III, G. D., "Pressure-Compensating Systems For Underwater Gas- Filled Electroacoustic Transducers," NRL Memorandum Report 2955, 1 December 1974.

Ivey, L. E., "Calibration of the J-15-9 at NRL/USRD Leesburg Facility and at the NUSC Seneca Lake Facility," NRL Memorandum Report 3643, November 1976.

Sherman, C. H., "Analysis of Acoustic Interactions in Transducer Arrays," *IEEE Transactions on Sonics and Ultrasonics*, vol. SU-13, no. 1, March 1966.

Sims, C. C., "High Fidelity Underwater Sound Transducers," *Proceedings of the IRE*, vol. 47, no. 5, May 1959.

Young, A. M., " Proposal for the Development of a High Power, Low Frequency Underwater Acoustic Source," NRL Memorandum Report 2897, 1 November 1974.

Young, A. M., "An Underwater Acoustic Source for the Infrasonic and Low-Audio-Frequency Range (USRD Type J13 Transducer)," NRL Report [illegible], 30 December 1975.

Appendix A

EQUATIONS DESCRIBING MOVING-COIL TRANSDUCER OPERATION

The basic equations describing moving-coil transducer operation are given below. For simple harmonic motion:

Deflection Amplitude:

$$\xi(\omega) = \frac{F}{K} \frac{1}{\sqrt{[1 - (\frac{\omega}{\omega_n})^2]^2 + [2d\frac{\omega}{\omega_n}]^2}} , \quad \text{(A-1)}$$

where

ξ = deflection amplitude
F = driving force (sinusoidal)
K = spring constant
ω = operating frequency
ω_n = resonance frequency
d = damping factor.

Acoustic power radiated from a small source:

$$P_A = U^2 R_r , \quad \text{(A-2)}$$

where

P_A = acoustic power
U = velocity amplitude
R_r = acoustic (radiation) resistance.

Radiation resistance for a piston in a small housing radiating into a solid angle:

$$R_r = \pi\omega^2\varrho_o \frac{a^4}{4c} , \quad \text{(A-3)}$$

where

ϱ_o = density of sea water
a = piston radius
c = velocity of sound.

The relationship between acoustic power and pressure at low frequencies:

$$P_A = (\frac{p^2}{\varrho_o c}) 4\pi r^2, \quad \text{(A-4)}$$

where

r = distance from source at which pressure is measured
p = pressure.

The force on a current-carrying conductor in a magnetic field:

$$F = B\ell i, \tag{A-5}$$

where

B = magnetic flux density
ℓ = length of coil wire
i = current.

Combining equations (A-2), (A-3), and (A-4), we obtain

$$p = \frac{U\omega\varrho_o a^2}{4r}. \tag{A-6}$$

To examine the relationship between current and pressure, it is necessary to evaluate equation (A-1) in three separate frequency regions .

Below resonance frequency $\left[\left(\frac{\omega}{\omega_n}\right)^2 << 1 \right]$,

$$\xi(\omega) = \frac{F}{K} \tag{A-7}$$

$$U(\omega) = \frac{d\xi}{dt} = \omega \frac{F}{K} \tag{A-8}$$

$$p = \frac{\omega^2 F \varrho_o a^2}{4Kr} \quad \text{(stiffness controlled).} \tag{A-9}$$

At resonance frequency $\left[\left(\frac{\omega}{\omega_n}\right)^2 = 1 \right]$,

$$\xi(\omega) = \frac{F}{2dK} \tag{A-10}$$

$$U(\omega) = \frac{\omega F}{2dK} \tag{A-11}$$

$$p = \frac{\omega F \varrho_o a^2}{4d_o r} \quad \text{(damping controlled),} \tag{A-12}$$

where

$$d_o = \text{damping} \left(d_o = \frac{2dK}{\omega_n} \right).$$

Above resonance frequency $\left[\left(\frac{\omega}{\omega_n}\right)^2 >> 1 \right]$,

$$\xi(\omega) = \frac{F}{\omega^2 m} \tag{A-13}$$

$$u(\omega) = \frac{F}{\omega m} \tag{A-14}$$

$$p = \frac{F \varrho_o a^2}{4mr} \quad \text{(mass controlled).} \tag{A-15}$$

Applying equation (A-5), we obtain

Below resonance: $$\frac{p}{i} = \frac{\omega^2 B \ell \varrho_o a^2}{4Kr} . \quad \text{(A-16)}$$

At resonance: $$\frac{p}{i} = \frac{\omega B \ell \varrho_o a^2}{4 d_o r} . \quad \text{(A-17)}$$

Above resonance: $$\frac{p}{i} = \frac{B \ell \varrho_o a^2}{4mr} . \quad \text{(A-18)}$$

The quantity p/i describes the transducer acoustic output response to a constant current input. It is called the transmitting current response (TCR). The response described by these expressions is shown in figure 1.

Expression (A-16) shows the response increasing with ω^2 or at a rate of 12 dB per octave. The response at resonance, according to equation (A-17), is determined by the damping, d_o. Above resonance, equation (A-18) indicates a flat response, the level of which is determined by flux density, coil wire length, sea water density, piston radius, and total mass.

Figure 1 shows some common disturbances in the theoretical response. At low frequencies, limiting the travel of the piston results in a 12 dB per octave slope. This is shown by applying the relationship between travel and velocity (equation (A-19)) to equation (A-6):

$$U = \omega \xi . \quad \text{(A-19)}$$

Therefore,

$$p = \frac{\omega^2 \xi \varrho_o a^2}{4r} , \quad \text{(A-20)}$$

which states that for constant travel, pressure will increase with the square of frequency.

The notch followed by a peak in the middle of the response is characteristic of a resonance mechanism occurring within the transducer, on its exterior, or in the path between the transducer and the receiver. The most common cause of this deviation is the resonance air path between the volume of air contained under the piston face and the volume of air contained in the compliance chamber (discussed later).

The disturbance at the high end of the response is caused by the piston dome "breaking up," or reaching the first mode of flexural vibration.

The transducer is normally operated in the frequency range between the fundamental resonance and the breakup frequency. Through careful design this range can be as great as 6 to 7 octaves of frequency. The fundamental resonance is determined by

$$\omega_n = \sqrt{\frac{1}{M_t C}} . \quad \text{(A-21)}$$

where

M_t = total mass

C = total mechanical compliance.

Total mass consists of the mass of the vibrating part of the transducer assembly and the mass of the water load on the dome. The water load, M_w, has been determined to be

$$M_w = 1.93 (\varrho_o a^3) , \tag{A-22}$$

where

a = piston radius.

The piston assembly mass, M_p, varies with design, but usually falls within

$$\varrho_o a^3 \leqslant M_p \leqslant 2\varrho_o a^3 . \tag{A-23}$$

Total compliance is comprised of the compliance of the spring assembly used to center the coil in the magnetic gap and the compliance of the contained air. Expression (A-21) then becomes

$$f = \frac{1}{2\pi} \sqrt{M_t \frac{1}{\frac{C_a C_s}{C_a + C_s}}} , \tag{A-24}$$

where

C_a = mechanical compliance of the contained air

C_s = mechanical compliance of the centering spring assembly,

which resolves into

$$f = \frac{1}{2} \pi \sqrt{\frac{1}{M_t C_s} + \frac{1}{M_t C_a}} , \tag{A-25}$$

or

$$f = \sqrt{f_a^2 + f_s^2} , \tag{A-26}$$

where

f_a = resonance frequency due to air compliance,

f_s = resonance frequency due to spring compliance.

The acoustical compliance of air is

$$C_{aA} = V_o/\gamma P_o(1 + \frac{h}{35})^2 \quad , \tag{A-27}$$

where

V_o = contained air volume at atmospheric pressure
P_o = atmospheric pressure
γ = ratio of the specific heats of air
h = depth in feet.

To perform the air resonance calculation, the acoustical mass $\frac{M_t}{A_P^2}$ is used in the expression

$$f_a = \frac{1}{2\pi}\left[\frac{1}{\frac{M_t}{A_P^2}(V_o/\gamma P_o(1 + \frac{h}{35})^2)}\right]^{1/2} , \tag{A-28}$$

where A_P is the area of the piston.

The resonance frequency due to the spring is

$$f_s = \frac{1}{2\pi}\sqrt{\frac{K_s}{M_t}} \quad , \tag{A-29}$$

where K_s is the stiffness of the spring.

Therefore, combining equations (A-26), (A-28), and (A-29), we get

$$f = \frac{1}{2\pi}\left[\frac{A_P^2\gamma P_o(1 + \frac{h}{35})^2}{M_t V_o} + \frac{K_s}{M_t}\right]^{1/2} .$$

Appendix B

EFFECT OF SCALING UP TRANSDUCER DIMENSIONS

With regard to the effect on performance of scaling up transducer dimensions, it has been shown that doubling the number of transducers will increase the total TCR by 6 dB. Assume a doubling in the volumetric dimensions of a single transducer so that

$$a' = 2^{1/3}a \tag{B-1}$$

$$h' = 2^{1/3}h \ , \tag{B-2}$$

where a = radius
h = cylindrical height

so that

$$2\pi a'^2 h' = 4\pi a^2 h \tag{B-3}$$

$$V' = 2V \ , \tag{B-4}$$

where V = volume.

To evaluate the effect on pressure,

$$p = \frac{B\ell i \varrho_o a^2}{4m_t r} \tag{B-5}$$

will be used.

Magnetic flux density will remain unchanged if magnetic air gap volume and magnetic material volume are both doubled.

Water load mass will be

$$M'_w = 1.93\,\varrho_o a'^3 = 1.93\,(2^{1/3}a)^3 = 2M_w \ . \tag{B-6}$$

Piston mass will also follow and total mass can be assumed to double. The change in (ℓi) is determined by assuming the same number of turns but with scaled-up wire size. This would permit the traditional two layers of windings to fill the air gap, and current will be scaled up with cross section to maintain the same maximum current density.*

$$i'_{max} = 2^{2/3} i_{max} \ . \tag{B-7}$$

The length of the coil would increase with circumference or radius, a:

$$\ell' = 2^{1/3}\ell \ . \tag{B-8}$$

*This is a highly simplified approach to current scaling; however, several other analyses involving pole piece eddy current calculations and total dissipated power calculations indicate a similar scaling factor.

When rewritten, equation (B-5) becomes

$$p'_{max} = \frac{B(2^{1/2})\ell(2^{1/2})i\varrho_o(2^{1/2})^2a^2}{4(2)m_t r} = 2^{1/2}p_{max}$$

$$= 1.56\,p_{max} \ . \qquad \text{(B-9)}$$

To equal the power of the two of the smaller transducers, a scaling factor of 3 is necessary:

$$p'' = 3^{1/2}p = 2p \ . \qquad \text{(B-10)}$$

If weight is not a problem, this solution offers the advantage of smaller size since the largest dimension is only 1.45 times that of the smaller unit rather than double, as in the dual unit.

Equation (A-20), below, is the expression for sound pressure level, p, as a function of angular frequency, ω; piston travel, ξ; piston radius, a; and media density, ϱ_o:

$$p = \frac{\omega^2\xi\varrho_o a^2}{4r}, \qquad \text{(A-20)}$$

where r is the distance at which the sound pressure level is measured.

The lowest frequency, ω_ℓ, at which maximum acoustic power can be produced occurs when

$$p = p_{max} \qquad \text{(B-11)}$$

and

$$\xi = \xi_{max} \ . \qquad \text{(B-12)}$$

p_{max} is determined by equation (B-9), above, and occurs when drive current cannot be increased without exceeding the safe transducer operating temperature. ξ_{max} occurs when the piston travel approaches the physical stops.

Rewriting equation (A-20), we obtain

$$\omega_\ell = \frac{2}{a}\left[\frac{p_{max}r}{\xi_{max}\varrho_o}\right]^{1/2} .$$

Using the scaled-up transducer, we obtain the lowest frequency, ω_ℓ, at which p_{max} may be generated:

$$\omega'_\ell = \frac{2}{2^{1/2}a}\left[\frac{p_{max}r}{2^{1/2}\xi_{max}\varrho_o}\right]^{1/2} = 2^{-1/2}\omega_\ell = 0.707\omega_\ell \ . \qquad \text{(B-13)}$$

The same value of ω'_ℓ occurs when two of the smaller transducers are operated simultaneously.

Appendix C

GLOSSARY OF SYMBOLS

Symbol	Meaning	Units
a	piston radius	m (meter)
A_p	piston area	m^2
B	magnetic flux density	weber/m^2
c	wave velocity	m/sec
C	total mechanical compliance	m/newton
C_a	mechanical compliance of air	m/newton
C_{aA}	acoustical compliance of air	m^5/newton
C_s	mechanical compliance of spring	m/newton
d	damping factor	kg/m/sec
d_o	damping	—
F	driving force (rms)	newton
f_a	resonance frequency, air	Hz
f_s	resonance frequency, spring	Hz
h	depth	m
i	current	ampere
K	spring constant	newton/m
ℓ	length of coil wire	m
m	mass	kg
M_p	mechanical piston assembly mass	kg
M_t	total mechanical mass	kg
M_W	mechanical water load mass	kg
p	sound pressure level (rms)	dB
P_A	acoustic power radiated	newton/m^2
P_o	atmospheric pressure	newton/m^2
p_{tcr}	transmitting current response	dB//μPa
r	distance from transducer	m
R_r	acoustic radiation resistance	kg/sec
U	particle velocity	m/sec
V_o	volume	m^3
γ	ratio of specific heats of air	
ξ	displacement	m
ξ_{max}	piston travel limit	—
ϱ_o	density of water	kg/m^3
ω	angular frequency	radian/sec
$\omega_n = \omega_o$	resonance angular frequency	radian/sec

INITIAL DISTRIBUTION LIST

Addressee	No. of Copies
ONR (M. Odeguard, LCDR Williams, A. Sykes)	3
DWTNSRDC CARD (J. O'Donnell, H. Pierce, G. Maybrey, J. Valentine, L. Avelyra, P. Rispin)	6
NRL (A. Gouda, B. Hurdle)	2
NRL, Orlando (J. Blue, T. Whelan, L. Ivey, M. Young, G. Hugus, M. Grady)	6
NORDA (R. Van Wyckhouse, C. Stuart, L. Solomon)	3
NAVELECSYSCOM, PME-124-2211 (R. Mountjoy), ELEX 320 (J. Sinsky, K. Myers, C. Brier) PME-124-60 (H. Ford, H. Cox, W. Dossinger)	7
NAVSEASYSCOM, SEA-063R (C. Walker, C. Smith)	2
NAVAIRDEVCEN, Key West (D. Probert)	1
NOSC (D. Carson, G. Pickens, J. Percy)	3
NOSC, Code 6565 (Library)	1
DTIC	12
Bolt Beranek & Newman, Inc., 50 Moulton St., Cambridge, MA 02138 (W. Hamblin, D. Gogus)	2
MAR, Inc., 1335 Rockville Pike, Rockville, MD 20852 (J. Diggs)	1
Planning Systems, Inc., 7900 Westpark Drive, Suite 600, McLean, VA 22102 (W. Dedman)	1
Western Electric Co., Dept. 7451, Guilford Center, Greensboro, SC 27420 (C. Schoonover, M. Grassia, A. Wallens)	3
Hydrotronics, Inc., 631 S. Brockhurst St., Anahiem, CA 92804 (Dr. S. Berlin)	1
Hydrotronics, Inc., 7926 Jones Branch Drive, McLean, VA 22101 (E. Nugent)	1
Hydrotronics, Inc., P.O. Box 21068, Ft. Lauderdale, FL 33335 (R. Judd, P. Fortin, W. Williams, G. Desmarais, A. Ferianc, W. Dale)	6
University of Miami, RSMAS, Rickenbacker Causeway, Miami, FL, 33149 (Dr. A. Meyerberg)	1
General Offshore Corp., 2605 Sterling Rd., Ft. Lauderdale, FL, 33315 (C. Gattos, M. Collier, J. Kennedy)	3
Palisades Geophysical, 615 SW 2nd Ave., Miami, FL 33130 (Technical Director)	1
Envo, Inc., 800 Follin Lane, Vienna, VA 22180 (C. Metheny)	1
A. D. Little Co., 25 Acorn Park, Cambridge, MA 02140 (W. Sykes)	1
Science Applications, Inc., 1710 Goodridge Drive, P.O. Box 1303, McLean, VA 22102 (P. Rost)	1
Dynamic Systems Inc., 8200 Greensboro Drive, Suite 500, McLean, VA 22102 (K. Hastie)	1
Ramcor, Inc., 800 Follin Lane, Vienna, VA 22180 (V. Davis)	1